NASA TMX 51474

24p

N65-89071
X64-12018*

Code 2A

(NASA TMX-51474)

NATIONAL AERONAUTICS AND SPACE ADMINISTRATION

PROPOSED JOURNAL ARTICLE

THE LAUNCHING OF SURFACE WAVES ON A CYLINDRICAL REACTIVE SURFACE

By Norman C. Wenger

31 Dec. 1963 24p refs

Submitted for Publication

6021505

NASA. Lewis Research Center
Cleveland, Ohio

NASA Centers Only.

Prepared for

Institute of Electrical and Electronic Engineers
Transactions on Antennas and Propagation

December 31, 1963

NASA Scientific and Technical Information Facility
NASA Centers Only
FOR SCIENTIFIC AND TECHNICAL INFORMATION
FACILITY COPY

THE LAUNCHING OF SURFACE WAVES ON A CYLINDRICAL REACTIVE SURFACE

By Norman C. Wenger*

Lewis Research Center
National Aeronautics and Space Administration
Cleveland, Ohio

12018

SUMMARY

The excitation of the dominant TM surface wave on a cylindrical reactive surface is discussed. The surface wave launcher consists of a perfectly conducting, infinitely thin cylindrical surface of radius b coaxial with a cylindrical reactive surface of a radius a where $b > a$. The reactive surface extends from $-\infty < z < \infty$, and the perfectly conducting surface extends from $-\infty < z \leq 0$. The incident field is the dominant TM mode in the coaxial portion of the structure propagating in the positive z-direction.

Numerical results are obtained for the reflected field, the surface wave field, and the radiation field. These results are then compared with the results that use two approximate aperture distributions.

This method of excitation was very efficient over a large range of frequencies and over wide variations in the surface reactance. AUTHOR

INTRODUCTION

The problem of exciting surface waves on various types of structures has been treated to a great extent in the literature.[1] A general requirement for a good surface wave launcher is that it have a high launching efficiency over a large frequency bandwidth. Brown[2] has shown that the launching efficiency of a finite-sized launcher can be made arbitrarily close to 100 percent. This large efficiency can be realized, however, only at the expense of frequency bandwidth.

---

*Member of IEEE.

The majority of numerical data presently available on launchers is for the class of launchers that are infinitesimal in some dimension. To this class belong the launchers in the form of short electric and magnetic current elements, line sources, current loops, slots, etc. Each of these sources can be characterized by a delta function in one or more of the coordinates. The case of the finite-sized aperture can be handled, at least in theory, by a superposition of infinitesimal sources. In practice, it is usually prohibitive to carry out this superposition, first, because of the complexity involved in the calculation and, second, because the aperture distribution may be unknown. In this case, the aperture distribution is often approximated by a "chopped" surface wave distribution; that is, the fields in the aperture plane are assumed to have the same form as the surface wave fields within the aperture and are assumed to vanish everywhere outside of the aperture. Another often used approximation method is Kirchhoff's approximation. In this method the aperture field is assumed to be of the same form as the unperturbed incident field. For either case the surface wave amplitude can be easily computed by an integration over the aperture plane since the surface wave modes and the radiation field are orthogonal.[3]

The purpose of this paper is to obtain rigorously the launching characteristics, radiation pattern, and frequency bandwidth for a finite-sized launcher. These results will then be compared with the results for the "chopped" surface wave distribution and with the results using Kirchhoff's approximation.

The structure to be considered is shown in figure 1. The structure consists of a reactive cylindrical surface of radius a and of infinite extent

in the z-direction. Coaxial with this cylinder is an infinitely thin, perfectly conducting surface of radius b for $z \leq 0$. The surface wave field, radiation field, and the reflected field will be computed when the incident field is the dominant TM mode in the region $a < r < b$, $z < 0$, propagating to the right.

FORMULATION OF THE PROBLEM

This problem falls into the class of two-part boundary value problems which can be handled by the Wiener-Hopf technique. The analysis will be carried out for a range in the parameters of the structure where only the dominant TM mode propagates in the region $a < r < b$, $z < 0$. In this case all of the field components can be derived from a scalar function $\psi(r,z)$ because of the circular symmetry of the structure. The function $\psi(r,z)$ is the θ component of the magnetic field.

In the region $a < r < b$, $z < 0$, $\psi(r,z)$ can be expanded in a series of the proper eigenfunctions:

$$\psi(r,z) = A_0^{\mp}\left[J_1(-jp_0r)H_0^2(-jp_0b) - J_0(-jp_0b)H_1^2(-jp_0r)\right]e^{\pm j\gamma_0 z}$$

$$+ \sum_{n=1}^{\infty} A_n^{\mp}\left[J_1(p_nr)H_0^2(p_nb) - J_0(p_nb)H_1^2(p_nr)\right]e^{\pm\gamma_n z} \qquad (1a)$$

where the A_n are complex constants. The eigenvalues p_n and the propagation constants γ_n satisfy the equations

$$jp_0a\,\frac{J_0(-jp_0b)H_0^2(-jp_0a) - J_0(-jp_0a)H_0^2(-jp_0b)}{J_1(-jp_0a)H_0^2(-jp_0b) - J_0(-jp_0b)H_1^2(-jp_0a)} = -\alpha a$$

$$p_n a \frac{N_0(p_n b)J_0(p_n a) - J_0(p_n b)N_0(p_n a)}{J_0(p_n b)N_1(p_n a) - N_0(p_n b)J_1(p_n a)} = \alpha a, \qquad n \geq 1$$

$$\alpha = kX_s/Z_0$$

$$\gamma_0^2 = p_0^2 + k^2$$

$$\gamma_n^2 = p_n^2 - k^2, \qquad n \geq 1$$

where k is the free-space wave number, X_s is the surface reactance, and Z_0 is the characteristic impedance of free space. The eigenfunctions in (1a) correspond to the TM_{0n} modes in the coaxial portion of the structure. The dominant TM_{00} mode will degenerate into a TEM mode as the surface reactance vanishes.

In the region $z > 0$, $r > a$, $\psi(r,z)$ will consist of a radiation field and a surface wave mode of the form

$$B_0 H_1^2(-jh_0 r)e^{-j\beta_0 z} \tag{1b}$$

where

$$jh_0 a \frac{H_0^2(-jh_0 a)}{H_1^2(-jh_0 a)} = \alpha a$$

and

$$\beta_0^2 = h_0^2 + k^2$$

The surface wave mode (1b) is the TM_0 mode or the Goubau wave. Only one subscript is necessary in denoting the surface wave modes since all of the modes have an evanescent character in the radial direction. A time variation for the field components of $e^{j\omega t}$ has been assumed.

It is convenient to decompose the total field $\psi_i(r,z)$ into two parts: an incident field $\psi_i(r,z)$ and a scattered field $\psi_s(r,z)$ where

$$\psi(r,z) = \psi_i(r,z) + \psi_s(r,z)$$

The incident field is the TM_{00} mode and will exist by definition for $a < r < b$ and all z.

$$\psi_i(r,z) \equiv \frac{\pi p_0 b}{2}\left[J_1(-jp_0r)H_0^2(-jp_0b) - J_0(-jp_0b)H_1^2(-jp_0r)\right]e^{-j\gamma_0 z} \qquad (2)$$

Since the incident field does not satisfy the proper boundary conditions for $z > 0$, the scattered field will be expected to contain a term of the same form as $\psi_i(r,z)$ for $z > 0$ to nullify this improper solution. The scattered field satisfies the following conditions:

$$\frac{\partial^2\psi_s}{\partial r^2} + \frac{1}{r}\frac{\partial\psi_s}{\partial r} + \frac{\partial^2\psi_s}{\partial z^2} + \left(k^2 - \frac{1}{r^2}\right)\psi_s = 0 \qquad (3)$$

$$\frac{1}{r}\frac{\partial}{\partial r}(r\psi_s) + \alpha\psi_s = 0, \qquad r = a, \text{ all } z \qquad (4)$$

$$\frac{1}{r}\frac{\partial}{\partial r}(r\psi_s) = 0, \qquad r = b, \qquad z < 0 \qquad (5)$$

$$\psi_s(b^+,z) - \psi_s(b^-,z) = e^{-j\gamma_0 z}, \qquad z > 0 \qquad (6)$$

$$\frac{1}{r}\frac{\partial}{\partial r}(r\psi_s)\bigg|_{r=b^+} - \frac{1}{r}\frac{\partial}{\partial r}(r\psi_s)\bigg|_{r=b^-} = 0 \qquad (7)$$

Equations (4) and (5) are a statement of the boundary conditions on the reactive surface and on the perfectly conducting surface, respectively. Equation (6) requires the scattered field to be discontinuous at $r = b$ by an amount equal to the discontinuity in the incident field, which thus makes the total field continuous. Equation (7) is equivalent to making the axial electric field continuous at $r = b$.

The solution for the scattered field can be formulated in terms of the

bilateral Laplace transformation of (3) along with the associated boundary conditions. Let

$$\varphi(r,\omega) \equiv \varphi^{+}(r,\omega) + \varphi^{-}(r,\omega)$$

where

$$\varphi^{+}(r,\omega) \equiv \int_{0}^{\infty} \psi_s(r,z)e^{-\omega z}\, dz$$

and

$$\varphi^{-}(r,\omega) \equiv \int_{-\infty}^{0} \psi_s(r,z)e^{-\omega z}\, dz$$

In order to make $\varphi^{+}(r,\omega)$ and $\varphi^{-}(r,\omega)$ analytic functions of ω in a common region in the ω-plane, the propagation constants γ_0 and β_0 are made complex. Let $j\gamma_0 = j\gamma_0' + \gamma_0''$ and $j\beta_0 = j\beta_0' + \beta_0''$ where γ_0', γ_0'', β_0', and β_0'' are real. In the final solution γ_0'' and β_0'' will be set equal to zero. Taking the transforms of (3), (4), and (5) gives

$$\frac{\partial^2\varphi}{\partial r^2} + \frac{1}{r}\frac{\partial\varphi}{\partial r} + \left(\omega^2 + k^2 - \frac{1}{r^2}\right)\varphi = 0 \tag{8}$$

$$\frac{1}{r}\frac{\partial}{\partial r}(r\varphi) + \alpha\varphi = 0, \qquad r = a \tag{9}$$

$$\frac{1}{r}\frac{\partial}{\partial r}(r\varphi^{-}) = 0, \qquad r = b \tag{10}$$

where ω has been restricted to the range $-\gamma_0'' < \mathrm{Re}\omega < \gamma_0''$. The solution to (8) that satisfies boundary condition (9) is

$$\varphi(r,\omega) = \varphi(b^{-},\omega)\,\frac{\left[\lambda H_0^2(\lambda a) + \alpha H_1^2(\lambda a)\right]J_1(\lambda r) - \left[\lambda J_0(\lambda a) + \alpha J_1(\lambda a)\right]H_1^2(\lambda r)}{\left[\lambda H_0^2(\lambda a) + \alpha H_1^2(\lambda a)\right]J_1(\lambda b) - \left[\lambda J_0(\lambda a) + \alpha J_1(\lambda a)\right]H_1^2(\lambda b)} \tag{11}$$

for

$$a < r < b$$

and

$$\varphi(r,\omega) = \varphi(b^+,\omega)\,\frac{H_1^2(\lambda r)}{H_1^2(\lambda b)} \tag{12}$$

for $r > b$ where $\lambda \equiv \sqrt{k^2 + \omega^2}$. The branch of λ where $\mathrm{Im}\,\lambda < 0$ must be selected to satisfy the radiation condition.

The unknown coefficients $\varphi(b^-,\omega)$ and $\varphi(b^+,\omega)$ in (11) and (12) can be determined by the discontinuity conditions on the scattered field at $r = b$. This can easily be accomplished by introducing the functions $J^+(b,\omega)$ and $J^-(b,\omega)$ where

$$J^+(b,\omega) \equiv \int_0^\infty \left[\psi_s(b^+,z) - \psi_s(b^-,z)\right] e^{-\omega z}\,dz$$

and

$$J^-(b,\omega) \equiv \int_{-\infty}^0 \left[\psi_s(b^+,z) - \psi_s(b^-,z)\right] e^{-\omega z}\,dz$$

$J^+(b,\omega)$ can be calculated at once by using (6).

$$J^+(\omega,b) = \frac{1}{\omega + j\gamma_0'}, \qquad \mathrm{Re}\,\omega > -\gamma_0' \tag{13}$$

From the definitions of $J^+(b,\omega)$ and $J^-(b,\omega)$ and (13) it is apparent that

$$\varphi(b^+,\omega) - \varphi(b^-,\omega) = J^-(b,\omega) + \frac{1}{\omega + j\gamma_0'} \tag{14}$$

Using boundary condition (10) gives

$$\frac{1}{r}\frac{\partial}{\partial r}(r\varphi) = \frac{1}{r}\frac{\partial}{\partial r}(r\varphi^+) \equiv \varphi^{+\prime}(b,\omega) \quad \text{for} \quad r = b$$

The coefficients $\varphi(b^-,\omega)$ and $\varphi(b^+,\omega)$ can now be expressed in terms of $\varphi^{+'}(b,\omega)$ and known functions of ω by performing the indicated differentiations with respect to r on (11) and (12). Substituting these results into (14) gives

$$\varphi^{+'}(b,\omega)F(\omega) = J^-(b,\omega) + \frac{1}{\omega + j\gamma_0} \tag{15}$$

where $F(\omega)$ is a known function of ω. The function $F(\omega)$ is written explicitly in the appendix along with its Wiener-Hopf factorization.

It is convenient to write $F(\omega)$ as a product of functions

$$F(\omega) = K(\omega)L(\omega)M(\omega)N(\omega)(\omega^2 + \gamma_0^2)^{-1} \tag{16}$$

where $K(\omega)$, $L(\omega)$, $M(\omega)$, and $N(\omega)$ are defined in the appendix. The function $F(\omega)$ can be put into the form

$$F(\omega) = F^+(\omega)/F^-(\omega)$$

by a Wiener-Hopf factorization where $F^+(\omega)$ is analytic and nonzero for $\mathrm{Re}\omega > -\gamma_0''$, and $F^-(\omega)$ is analytic and nonzero for $\mathrm{Re}\omega < \gamma_0''$. In the notation of (16), $F^+(\omega)$ and $F^-(\omega)$ can be expressed as

$$F^+(\omega) = p(\omega)K^+(\omega)L^+(\omega)M^+(\omega)N^+(\omega)(\omega + j\gamma_0)^{-1}$$

$$F^-(\omega) = p(\omega)K^-(\omega)L^-(\omega)M^-(\omega)N^-(\omega)(\omega - j\gamma_0)$$

where $p(\omega)$ is analytic everywhere in the finite ω-plane. The function $p(\omega)$ must be selected to give $F^+(\omega)$ and $F^-(\omega)$ algebraic behavior rather than exponential behavior at infinity. It can be shown that the asymptotic forms of $F^+(\omega)$ and $F^-(\omega)$ are

$$\begin{aligned} F^+(\omega) &= O(\omega^{-1/2}) \quad \text{as} \quad \omega \to \infty \\ F^-(\omega) &= O(\omega^{1/2}) \quad \text{as} \quad \omega \to -\infty \end{aligned} \tag{17}$$

Equation (15) can now be rewritten in the form

$$F^+(\omega)\varphi^{+\prime}(b,\omega) - \frac{F^-(-j\gamma_0)}{\omega + j\gamma_0} = \frac{F^-(\omega) - F^-(-j\gamma_0)}{\omega + j\gamma_0} + F^-(\omega)J^-(b,\omega) \qquad (18)$$

The left side of (18) is analytic for $\mathrm{Re}\omega > -\gamma_0''$, and the right side is analytic for $\mathrm{Re}\omega < \gamma_0''$. The equality in (18) holds only in the region $-\gamma_0'' < \mathrm{Re}\omega < \gamma_0''$. Figure 2 shows the regions in the complex ω-plane where the various transforms are analytic.

The solution for the scattered field is not unique unless the edge conditions are specified at $r = b$, $z = 0$.[4] These conditions require the axial component of the electric field to be of the order $z^{-1/2}$ at the edge, which makes the transform of the electric field (i.e., $\varphi^{+\prime}(b,\omega)$) of the order $\omega^{-1/2}$ as $\omega \to \infty$. A similar condition exists for the asymptotic form of the current at the edge. This condition requires $J^-(b,\omega)$ to be of the order ω^{-1} as $\omega \to -\infty$. Substituting these results into (18) shows that each side of (18) approaches zero as ω goes to infinity in the proper half plane. Thus, on applying Liouville's theorem, (18) can be equated to zero. Setting the left side equal to zero gives

$$\varphi^{+\prime}(b,\omega) = \frac{F^-(-j\gamma_0)}{F^+(\omega)(\omega + j\gamma_0)} \qquad (19)$$

Note that the proper edge conditions are satisfied in (19).

EVALUATION OF SCATTERED FIELDS

The function $\varphi^{+\prime}(b,\omega)$ in (19) can be computed in terms of $\varphi(b^-,\omega)$ from (11) or in terms of $\varphi(b^+,\omega)$ from (12). Using (11) gives

$$\varphi(b^-,\omega) = \frac{H_1^2\left(\sqrt{k^2 + \omega^2}\, b\right)F^-(-j\gamma_0)}{\sqrt{k^2 + \omega^2}\, H_0^2\left(\sqrt{k^2 + \omega^2}\, b\right)F^+(\omega)(\omega + j\gamma_0)} - \frac{F^-(-j\gamma_0)}{F^-(\omega)(\omega + j\gamma_0)} \qquad (20)$$

The scattered field, evaluated at $r = b$, can now be found by inverting (20).

$$\psi_s(b^-,z) = \frac{1}{2\pi j}\int_C \varphi(b^-,\omega)e^{\omega z}\,d\omega$$

The inversion contour C must be in the region $-\gamma_0'' < \mathrm{Re}\omega < \gamma_0''$ as shown in figure 3 and be on the proper sheet of the Riemann surface. The branch cuts were selected as straight lines extending radially from the branch points.

For $z < 0$ the contour can be closed in the right half ω-plane with a semicircle of infinite radius, which is deformed around the branch cut. The contribution to the integral along the semicircle and branch cut is zero. Thus, $\psi_s(b^-,z)$ can be expressed in terms of the residues of $\varphi(b^-,\omega)$ for $z < 0$. The poles of $\varphi(b^-,\omega)$ are due to the zeros of $F^-(\omega)$ for $\mathrm{Re}\omega > -\gamma_0''$. In the notation of (16) all of the zeros of $F^-(\omega)$ are contained in the term $N^-(\omega)(\omega - j\gamma_0)$. The zero at $\omega = j\gamma_0$ corresponds to the dominant TM_{00} mode, and the zeros at $\omega = \gamma_n$ correspond to the higher order TM_{0n} modes. For $z \ll 0$, $r = b^-$, the scattered field will consist of only the TM_{00} reflected mode since the TM_{on} $(n \geq 1)$ modes are evanescent. Thus,

$$\psi_s(b^-,z) = \frac{F^-(-j\gamma_0)e^{j\gamma_0 z}}{2j\gamma_0 p(j\gamma_0)K^-(j\gamma_0)L^-(j\gamma_0)M^-(j\gamma_0)N^-(j\gamma_0)} \qquad (21)$$

for $z \ll 0$. The radial dependence of the scattered field for $a < r < b$, $z < 0$, has already been determined in (1a).

The scattered field for $z > 0$ can be found by closing the contour with a semicircle of infinite radius in the left half ω-plane. Again, the contour must be deformed around the branch cut. For $z > 2(b - a)$ the contribu-

tion to the integral along the semicircle is zero. Therefore, the scattered field can be evaluated in terms of the residues of $\varphi(b^-,\omega)$ and the branch cut integral. The function $\varphi(b^-,\omega)$ has two poles for $\mathrm{Re}\omega < \gamma_0''$. The surface wave pole is located at $\omega = -j\beta_0$, and a second pole, located at $\omega = -j\gamma_0$, gives rise to a field that cancels the incident field for $z > 0$. In the notation of (16) the surface wave pole corresponds to a zero of $M^+(\omega)$, and the pole at $\omega = -j\gamma_0$ appears explicitly in $\varphi(b^-,\omega)$. Evaluating the residues gives

$$\psi_s(b^-,z) = \frac{jH_1^2(-jh_0b)F^-(-j\gamma_0)e^{-j\beta_0 z}}{\beta_0\left(2 + \alpha a - \frac{h^2 a}{\alpha}\right) H_0^2(-jh_0b)p(-j\beta_0)K^+(-j\beta_0)L^+(-j\beta_0)M^-(-j\beta_0)N^+(-j\beta_0)} - e^{-j\gamma_0 z} + \text{Branch cut integral} \qquad (22)$$

for $z > 2(b - a)$. The first term on the right in (22) corresponds to the TM_0 surface wave. The radial dependence of the surface wave mode has been determined in (1b). The second term cancels the incident field for $z > 0$ since $\psi_i(b^-,z) \equiv e^{-j\gamma_0 z}$.

The scattered field for $r > b$ can be found by evaluating $\varphi^{+\prime}(b,\omega)$ from (12) and substituting the result into (19). The result is

$$\psi_s(r,z) = \frac{1}{2\pi j}\int_C \frac{H_1^2\left(\sqrt{k^2 + \omega^2}\, r\right)F^-(-j\gamma_0)e^{\omega z}}{\sqrt{k^2 + \omega^2}\, H_0^2\left(\sqrt{k^2 + \omega^2}\, b\right)F^+(\omega)(\omega + j\gamma_0)}\, d\omega \qquad (23)$$

for $r > b$. The asymptotic form of the radiated field can be determined by saddle-point integration. This integration can be easily carried out by a suitable change in the variable of integration and a transformation of r and z into spherical coordinates. Let $\omega = -jk \sin \nu$ where

$\nu = \sigma + j\eta$, $r = \rho \cos \varphi$, and $z = \rho \sin \varphi$ (see fig. 1). With these changes (23) becomes

$$\psi_s(\rho,\varphi) = -\frac{1}{2\pi j}\int_{C'} \frac{H_1^2(k\rho \cos\varphi \cos\nu)F^-(-j\gamma_0)e^{-jk\rho \sin\varphi \sin-\nu}}{H_0^2(kb \cos\nu)F^+(-jk \sin\nu)(\gamma_0 - k \sin\nu)}\, d\nu \qquad (24)$$

If the contour C' does not pass through a point where $\cos\nu = 0$, and if $\cos\varphi \neq 0$, then for sufficiently large $k\rho$ the Hankel function $H_1^2(k\rho \cos\varphi \cos\nu)$, in (24) can be replaced by its asymptotic form

$$H_1^2(k\rho \cos\varphi \cos\nu) \simeq \sqrt{\frac{2}{k\rho\pi \cos\varphi \cos\nu}}\, e^{-j\left(k\rho \cos\varphi \cos\nu - \frac{3\pi}{4}\right)}$$

where terms of the order $(k\rho)^{-3/2}$ and lower have been neglected. The scattered field is now given by

$$\psi_s(\rho,\varphi) = -\frac{1}{2\pi j}\int_{C'} \frac{2^{1/2}F^-(-j\gamma_0)e^{-j\left(k\rho \cos(\nu-\varphi) - \frac{3\pi}{4}\right)}\, d\nu}{H_0^2(kb \cos\nu)F^+(-jk \sin\nu)(\gamma_0 - k \sin\nu)(k\rho\pi \cos\varphi \cos\nu)^{1/2}} \qquad (25)$$

for $(k\rho) \gg 1$. The steepest descent contour C' (fig. 4) passes through the saddle point $\nu = \varphi$ and, in general, satisfies the equation $\mathrm{Re}[k \cos(\nu - \varphi)] = \mathrm{Re}\,k$. As the observation angle φ approaches $\pi/2$ the contour C' will cross the surface wave pole. For this range of φ the surface wave must be included in the expression for the total scattered field. The integral in (25) can be evaluated by expanding the exponent in a Taylor series about $\nu = \varphi$ and retaining only the first two terms. The result is

$$\psi_s(\rho,\varphi) = \frac{F^-(-\gamma_0)e^{-j(k\rho+\pi/2)}}{\pi F^+(-jk \sin\varphi)H_0^2(kb \cos\varphi)(\gamma_0 - k \sin\varphi)(k\rho \cos\varphi)} \qquad (26)$$

for $(k\rho) \gg 1$. It should be noted at this point that the function $\psi_s(r,z)$ is the θ component of the magnetic field in cylindrical coordinates. When the change was made to spherical coordinates, the form of the scattered field did not have to be modified since the θ components of a vector expressed in cylindrical and spherical coordinates are identical.

The radiated field as expressed in (26) is of the general form

$$\psi_s(\rho,\varphi) = G(\varphi) \frac{e^{-jk\rho}}{k\rho} \tag{27}$$

If more terms were retained in the asymptotic expansion of the Hankel function and in the expansion of the exponent in (25), $\psi_s(\rho,\varphi)$ would contain terms of the order $(k\rho)^{-3/2}$ and lower. The additional terms would give a better approximation for the radiated field, but they would not contribute any net radiated power. The flow of energy in the structure can be determined entirely from the amplitudes of the modes computed in (21) and (22) and from the radiated field as given in (26).

RESULTS

The amplitudes of the various modes were computed on an IBM 7094. Some typical results are shown in figures 5 to 8. The ratios of surface wave power, reflected power, and radiated power to incident power are shown as functions of kd where $d \equiv b - a$. The range of kd is restricted so that only the TM_{00} mode will propagate in the coaxial portion of the structure. The results show that this structure is very efficient in launching surface waves even when the surface reactance is quite low. It is also broad banded as evidenced by the small reflected power over a large range of kd.

The curves for the radiation pattern have been normalized by setting

the maximum value of the power density in the forward direction equal to 1. The radiation field approaches zero as the observation angle φ approaches $\pi/2$, at least to the first order in $(k\rho)^{-1}$. This phenomenon is referred to by Kane as the Karp-Karal lemma. In the back direction, the radiation pattern becomes singular as φ approaches $-\pi/2$. It can be shown that $G(\varphi)$, defined in (27), is of the form

$$G(\varphi) \simeq \frac{A}{\left(\frac{\pi}{2} + \varphi\right) \ln\left[\frac{\gamma kb}{2}\left(\frac{\pi}{2} + \varphi\right)\right]}$$

for $|\pi/2 + \varphi| \ll 1$. The same type of singularity is also present in the radiation pattern of a circular wave guide when the incident field is the TM_{01} mode.[5] The radiation patterns for other values of surface reactance are quite similar to that shown in figure 8. As the surface reactance is increased the beam width becomes slightly smaller for a fixed value of kd.

Figure 9 shows the launching efficiency vs. kd for the structure. Exact results are presented along with the results using Kirchhoff's approximation and the "chopped" surface wave distribution. The approximation techniques give quite accurate results for $kd > 1$. The values of kd when the approximations fail also give a large reflected power as shown in figure 5. The launcher would not be useful in this range of kd unless some impedance matching technique were employed. The launching characteristics, both exact and approximate, for other values of surface reactance have the same general behavior as those shown in figure 9. In all cases, the "chopped" surface wave distribution was found to be a better approximation than Kirchoff's approximation.

APPENDIX

The function $F(\omega)$ is expressed, for convenience, as the product of functions

$$F(\omega) \equiv K(\omega)L(\omega)M(\omega)N(\omega)(\omega^2 + \gamma_0^2)^{-1}$$

where

$$K(\omega) \equiv \frac{K^+(\omega)}{K^-(\omega)} \equiv \frac{2j}{\pi b \lambda}$$

$$L(\omega) \equiv \frac{L^+(\omega)}{L^-(\omega)} \equiv \frac{H_0^2(\lambda a)}{H_0^2(\lambda b)}$$

$$M(\omega) \equiv \frac{M^+(\omega)}{M^-(\omega)} \equiv \lambda + \alpha \frac{H_1^2(\lambda a)}{H_0^2(\lambda a)}$$

$$N(\omega) \equiv \frac{N^+(\omega)}{N^-(\omega)} \equiv$$

$$\frac{(\omega^2 + \gamma_0^2)}{\lambda^2\left[H_0^2(\lambda a)J_0(\lambda b) - H_0^2(\lambda b)J_0(\lambda a)\right] + \lambda\alpha\left[H_1^2(\lambda a)J_0(\lambda b) - H_0^2(\lambda b)J_1(\lambda a)\right]}$$

and

$$\lambda \equiv \sqrt{k^2 + \omega^2}$$

It is not necessary to compute both $K^+(\omega)$ and $K^-(\omega)$ since if, for example, $K^-(\omega)$ is known, then $K^+(\omega)$ can be obtained from its definition $K^+(\omega) \equiv K(\omega)K^-(\omega)$. $K^+(\omega)$ can also be obtained from the relation $K^+(\pm\omega)K^-(\mp\omega) = 1$ since $K(\omega)$ is an even function of ω. The same is true for $L(\omega)$, $M(\omega)$, and $N(\omega)$ since they are all even functions of ω. $K^-(\omega)$ can easily be determined by inspection giving

$$K^-(\omega) = (\pi b/2j)^{1/2}(\omega - jk)^{1/2}$$

The functions $L^-(\omega)$ and $M^-(\omega)$ can be found by applying Cauchy's integral formula to a strip in the complex ω-plane. The functions $L^-(\omega)$ and $M^-(\omega)$ can not be expressed in terms of elementary functions, but they can be written in the integral forms:[6]

$$L^-(\omega) = \exp\left[\frac{(\omega^2 + k^2)}{2\pi k}\,\text{P.V.}\int_1^\infty \frac{\ln \dfrac{H_0^2(-jka\sqrt{x^2-1})H_0^2(jkb\sqrt{x^2-1})}{H_0^2(jka\sqrt{x^2-1})H_0^2(-jkb\sqrt{x^2-1})}}{(x^2-1)(jkx-\omega)}\,dx\right]$$

$$M^-(\omega) = M^-(0)\exp\left[\int_0^\omega \left\{\frac{1}{2(s-jk)} - \frac{1}{s-j\beta_0}\right\}ds - \frac{k}{2\pi}\,\text{P.V.}\int_0^\omega\left\{\int_1^\infty \frac{(m^+(x)-m^-(x))dx}{jkx-s}\right\}ds\right]$$

where P.V. denotes the principal value of the integral and

$$m^\pm(x) \equiv \left[\frac{jkxa^2}{\pm\xi}\right]\cdot\left[\pm\xi - \alpha a\frac{H_1^2(\mp\xi)}{H_0^2(\mp\xi)}\right]^{-1}\cdot\left[1 + \alpha a \pm \frac{\alpha a}{\xi}\frac{H_1^2(\mp\xi)}{H_0^2(\mp\xi)} + \alpha a\left\{\frac{H_1^2(\mp\xi)}{H_0^2(\mp\xi)}\right\}^2\right]$$

$$\xi \equiv jka\sqrt{x^2-1}$$

The function $N(\omega)$ can be factored by expressing it as an infinite product. This is possible since $N(\omega)$ is an even function of $\sqrt{k^2+\omega^2}$ and has singularities in the form of simple poles.[7] The result is

$$N^-(\omega) = \sqrt{\frac{2j\alpha}{p_0^2\pi a}}\prod_{n=1}^{\infty}\left[\frac{\gamma_n - \omega}{p_n}\right]e^{+\frac{\omega d}{n\pi}}$$

The function $p(\omega)$ must be selected to give $F^+(\omega)$ and $F^-(\omega)$ algebraic behavior as $|\omega| \to \infty$. The proper $p(\omega)$ is

$$p(\omega) = \exp - \left[- \frac{\omega P}{2\pi k} + \frac{j\omega d}{2} + \frac{\omega d}{\pi} \ln \left(\frac{kd}{2\pi} \right) - \frac{\omega d}{\pi} + \frac{\gamma \omega d}{\pi} \right]$$

where γ is Euler's constant and

$$P \equiv P.V. \int_1^{\infty} \frac{\ln \left[\frac{H_0^2(-jka\sqrt{x^2-1}) H_0^2(jkb\sqrt{x^2-1})}{H_0^2(jka\sqrt{x^2-1}) H_0^2(-jkb\sqrt{x^2-1})} \right] - 2kd\sqrt{x^2-1}}{x^2-1} dx$$

FOOTNOTES

1. See for example: H. M. Barlow and J. Brown, "Radio Surface Waves," Oxford University Press, London, Chapters 9, 10, 11; 1962.

2. J. Brown, "Some Theoretical Results for Surface Wave Launchers," IRE Trans. on Antennas and Propagation, vol. AP-7, pp. S169-S174; December 1959.

3. R. E. Collin, "Field Theory of Guided Waves," McGraw-Hill Book Co., Inc., New York, N.Y., pp. 483-485; 1960.

4. B. Noble, "Methods Based on the Wiener-Hopf Technique," Pergamon Press, London, pp. 75-76; 1958.

5. N. Marcuvitz, ed. "Waveguide Handbook," McGraw-Hill Book Co., Inc., New York, N.Y., pp. 196-201; 1951.

6. For a description of this technique see: P. M. Morse and H. Feshbach, "Methods of Theoretical Physis," vol. 1, McGraw-Hill Book Co., Inc., New York, N.Y., pp. 987-989; 1953.

7. P. M. Morse and H. Feshbach, op.cit., pp. 384-385.

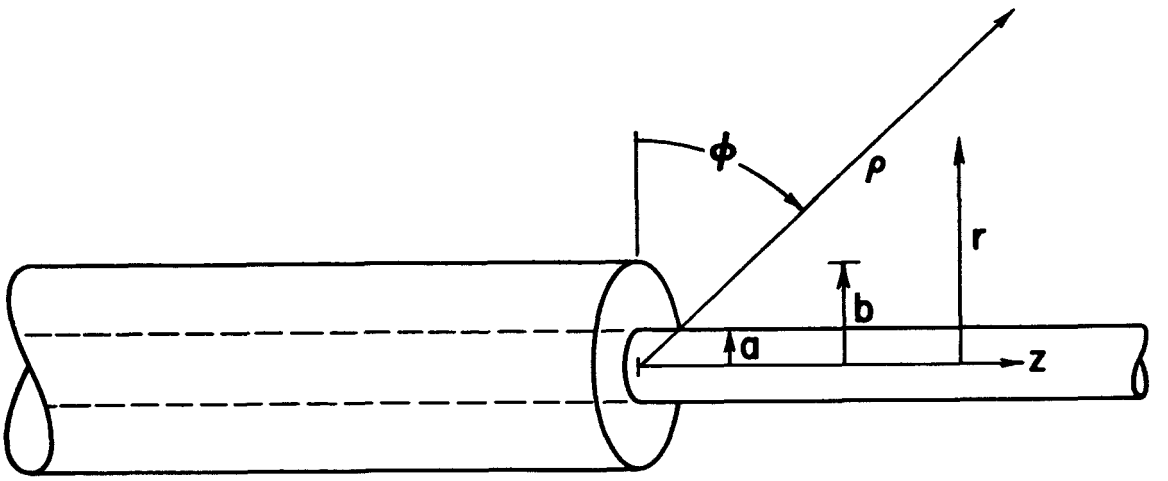

Figure 1. - Surface wave structure.

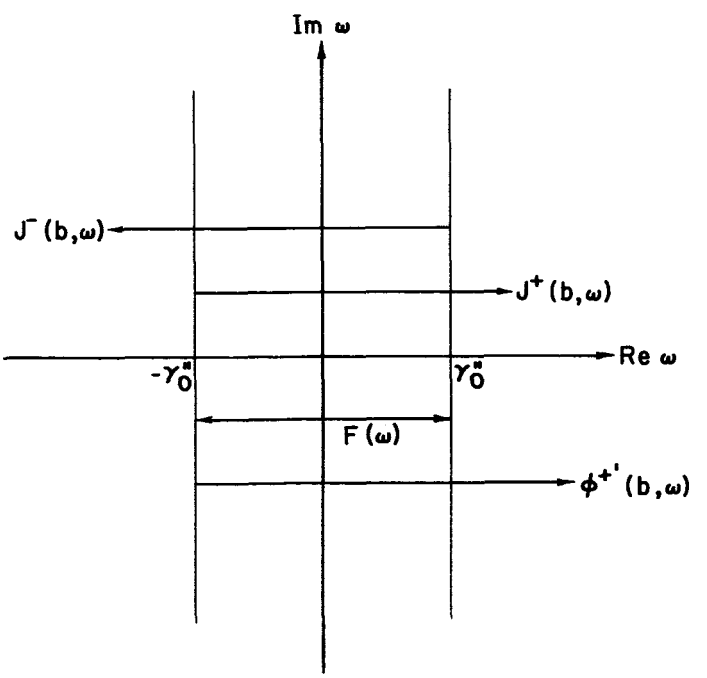

Figure 2. - Regions in complex ω-plane where transforms are analytic.

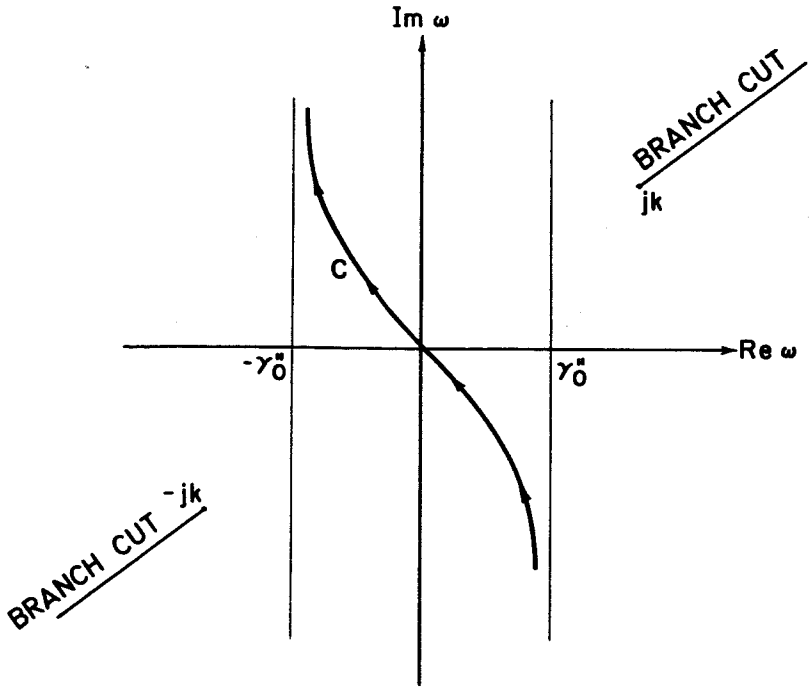

Figure 3. - The inversion contour in the complex ω-plane.

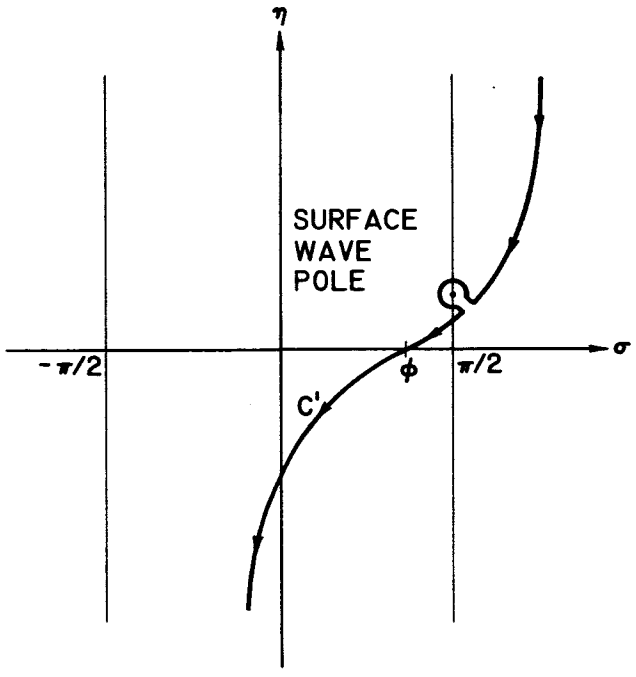

Figure 4. - The steepest descent contour in the complex ν-plane.

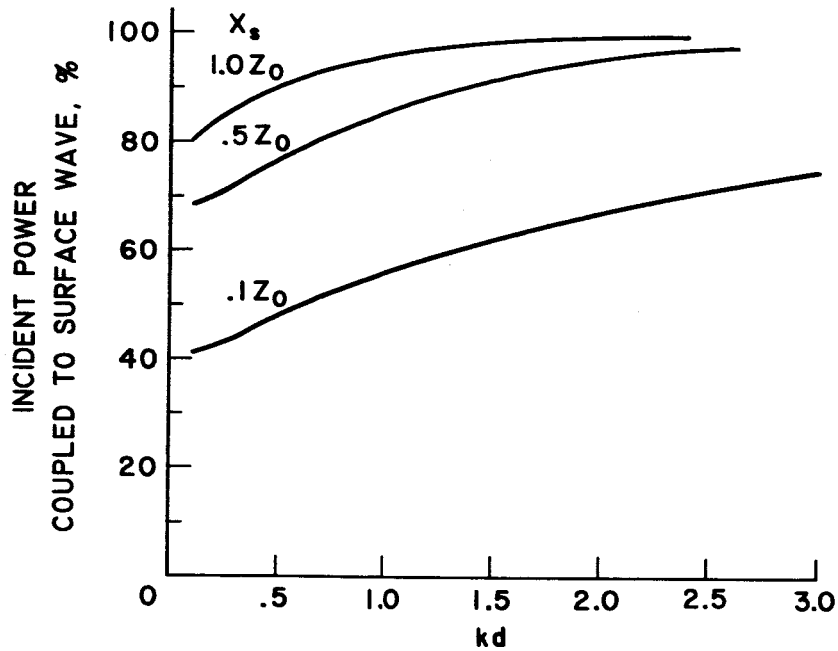

Figure 5. - Percentage of incident power coupled to the surface wave vs. kd for constant values of surface reactance X_S; b/a, 2.3.

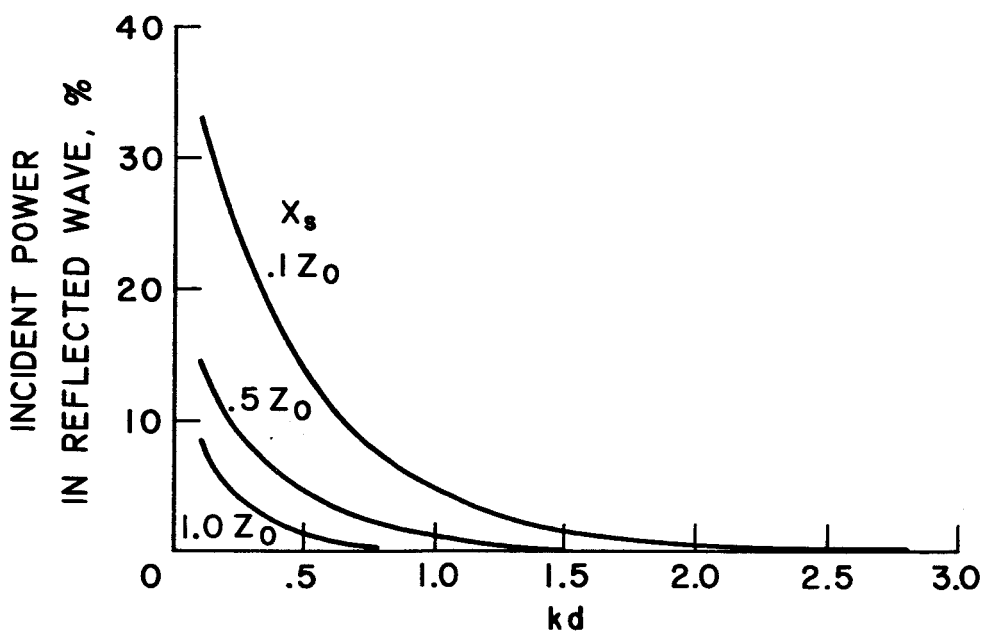

Figure 6. - Percentage of incident power coupled to the reflected wave vs. kd for constant values of surface reactance X_S; b/a, 2.3.

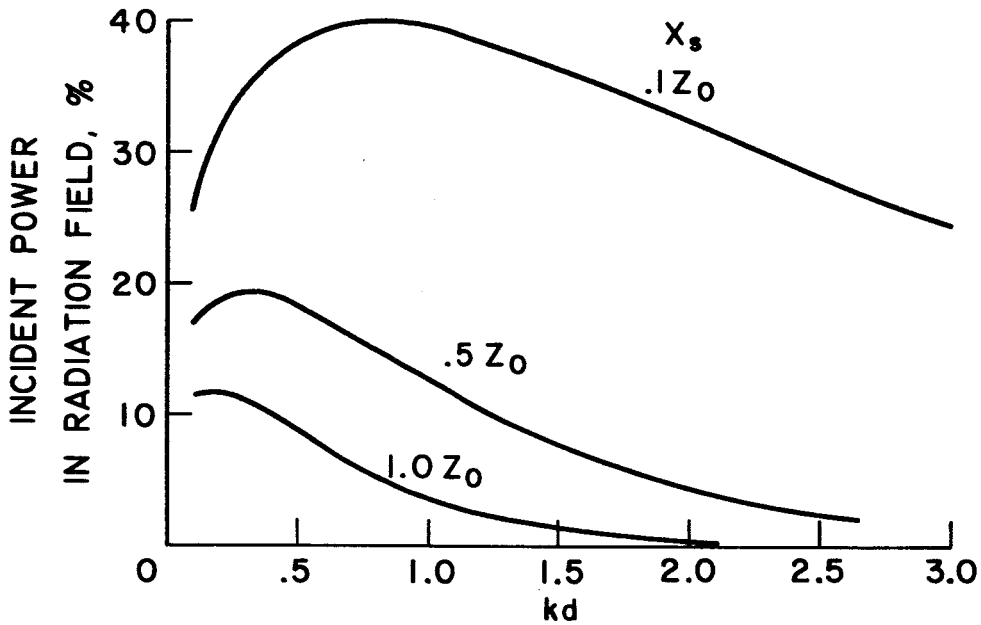

Figure 7. - Percentage of incident power coupled to the radiated wave vs. kd for constant values of surface reactance X_s; b/a, 2.3.

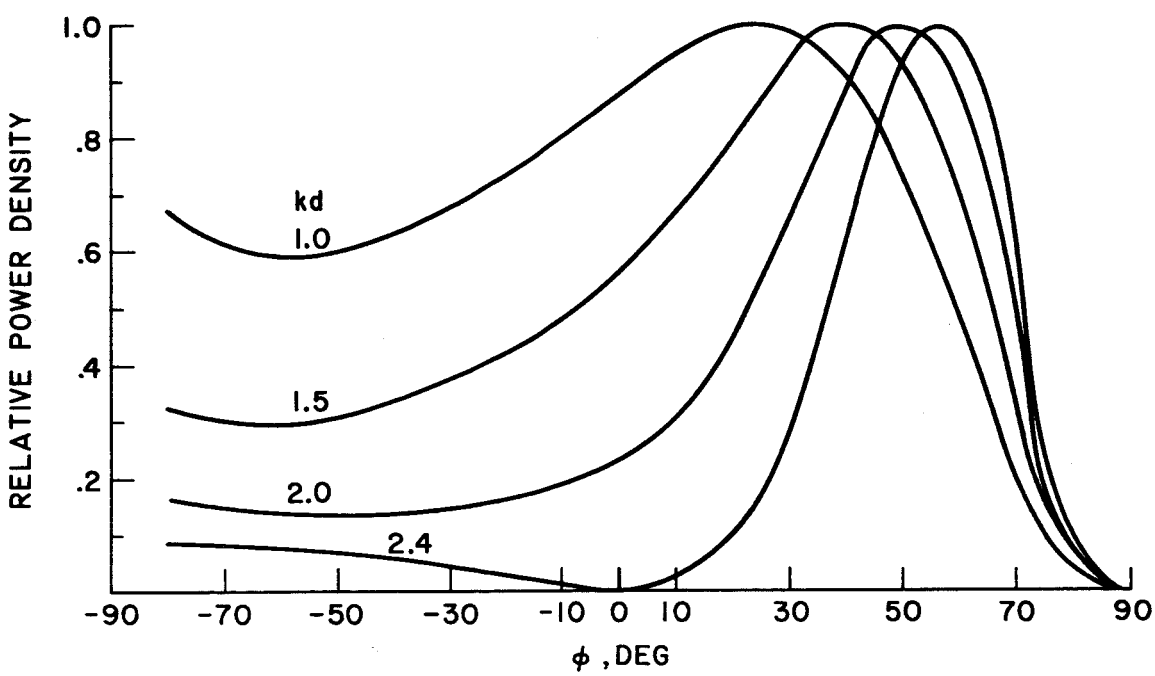

Figure 8. - The radiation pattern; X_s, 1.0 Z_0; b/a, 2.3.

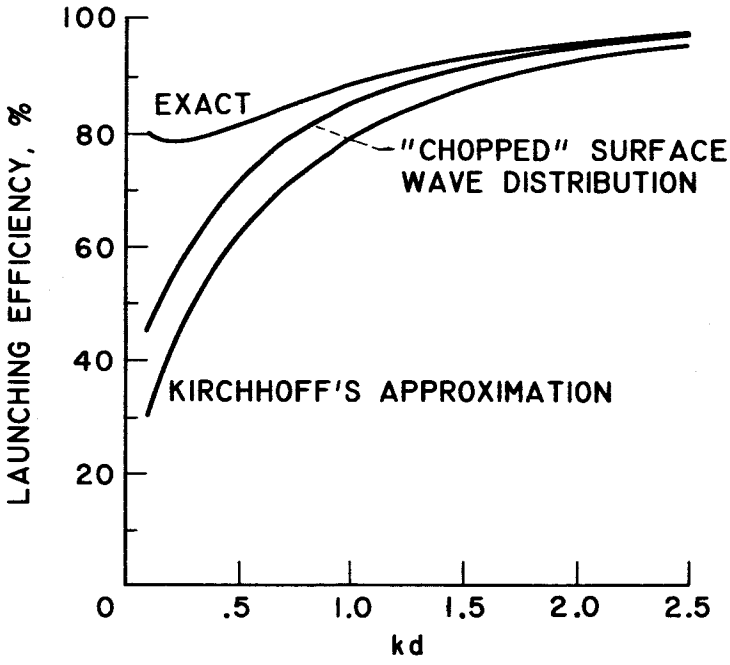

Figure 9. - Launching efficiency vs. kd; X_s, 0.5; b/a, 2.3.